ISSN 1948-0210 (online)

World Journal of *Stem Cells*

World J Stem Cells 2020 January 26; 12(1): 1-99

Published by Baishideng Publishing Group Inc

WJSC

World Journal of Stem Cells

Contents

Monthly Volume 12 Number 1 January 26, 2020

World Journal of Stem Cells
Volume 12 Number 1 January 26, 2020

Contents

NAME OF JOURNAL
World Journal of Stem Cells

ISSN
ISSN 1948-0210 (online)

LAUNCH DATE
December 31, 2009

FREQUENCY
Monthly

EDITORS-IN-CHIEF
Tong Cao, Shengwen Calvin Li, Carlo Ventura

EDITORIAL BOARD MEMBERS
https://www.wjgnet.com/1948-0210/editorialboard.htm

EDITORIAL OFFICE
Jin-Lei Wang, Director

PUBLICATION DATE
January 26, 2020

INSTRUCTIONS TO AUTHORS
https://www.wjgnet.com/bpg/gerinfo/204

GUIDELINES FOR ETHICS DOCUMENTS
https://www.wjgnet.com/bpg/GerInfo/287

GUIDELINES FOR NON-NATIVE SPEAKERS OF ENGLISH
https://www.wjgnet.com/bpg/gerinfo/240

PUBLICATION MISCONDUCT
https://www.wjgnet.com/bpg/gerinfo/208

ARTICLE PROCESSING CHARGE
https://www.wjgnet.com/bpg/gerinfo/242

STEPS FOR SUBMITTING MANUSCRIPTS
https://www.wjgnet.com/bpg/GerInfo/239

ONLINE SUBMISSION
https://www.f6publishing.com

World Journal of Stem Cells

Submit a Manuscript: https://www.f6publishing.com

World J Stem Cells 2020 January 26; 12(1): 35-54

DOI: 10.4252/wjsc.v12.i1.35

ISSN 1948-0210 (online)

ORIGINAL ARTICLE

Basic Study

Sphere-forming corneal cells repopulate dystrophic keratoconic stroma: Implications for potential therapy

Himanshu Wadhwa, Salim Ismail, Jennifer J McGhee, Bert Van der Werf, Trevor Sherwin

ORCID number: Himanshu Wadhwa (0000-0002-3287-4453); Salim Ismail (0000-0002-6644-9615); Jennifer J McGhee (0000-0001-7488-9250); Bert Van der Werf (0000-0003-3072-5937); Trevor Sherwin (0000-0002-9090-1034).

Author contributions: Wadhwa H and Ismail S participated in the experimental design, data acquisition analysis and manuscript writing; McGhee JJ participated in experimental design and cell and tissue preparation; Van der Werf B participated in data analysis and manuscript writing; Sherwin T participated in study design, experimental design and manuscript writing; All authors read, edited and approved the final manuscript.

Supported by Save Sight Society of New Zealand, No. 37116543; New Zealand Wound Care Society, No. 3713325; John Hamel MacGregor Trust.

Institutional review board statement: This study was conducted under ethical approval by the Northern X Regional Ethics Committee and since reviewed by the Northern A Health and Disability Ethics Committee (New Zealand). Ethics reference: NTX/07/08/080/AM06

Conflict-of-interest statement: Prof. Sherwin reports grants from Save Sight Society of New Zealand, grants from Auckland Medical Research Foundation, grants from New Zealand Wound Care Society, and grants from John Hamel MacGregor Trust during the

Himanshu Wadhwa, Salim Ismail, Jennifer J McGhee, Trevor Sherwin, Department of Ophthalmology, Faculty of Medical and Health Sciences, The University of Auckland, Auckland 1023, New Zealand

Bert Van der Werf, Department of Epidemiology and Biostatistics, School of Population Health, Faculty of Medical and Health Sciences, The University of Auckland, Auckland 1023, New Zealand

Corresponding author: Trevor Sherwin, PhD, Professor, Department of Ophthalmology, Faculty of Medical and Health Sciences, The University of Auckland, Private Bag 92019, Auckland 1023, New Zealand. t.sherwin@auckland.ac.nz

Abstract

BACKGROUND

Keratoconus is a degenerative corneal disease characterised by aberrant cell behaviour and loss of matrix that can result in vision loss. Cells extracted from peripheral corneas can form stem cell-enriched spheres, which have shown the potential to repopulate the normal peripheral corneal stroma *in vitro* upon sphere implantation but have not been previously studied in keratoconic tissue.

AIM

To investigate the therapeutic potential of stem cell-enriched spheres formed from extracted peripheral human corneal cells when introduced to keratoconic tissue.

METHODS

Stem cell-enriched spheres were formed from extracts of normal cadaveric human peripheral corneal cells. These spheres were implanted into incisions created in full thickness and onto the surface of 10 μm thin sections of keratoconic and normal stromal tissues *in vitro*. Tissue sections were used to maximise use of limited keratoconic tissue available for research. Living cells were stained with Calcein-AM and visualised with stereo and fluorescence microscopy to assess survival and behaviours between the time of implantation day 0 and 14 d (D14) from implantation. Sphere cells in implanted tissues were characterised for stem cell and differentiation markers using immunohistochemistry and droplet digital PCR to assess the potential implications of these characteristics in the use of spheres in keratoconus treatment.

RESULTS

Spheres were successfully implanted into full-thickness central corneal tissue and

conduct of the study.

Data sharing statement: The datasets used and/or analysed during the current study are available from the corresponding author on reasonable request.

Manuscript source: Unsolicited manuscript

Received: June 25, 2019
Peer-review started: June 29, 2019
First decision: July 31, 2019
Revised: September 11, 2019
Accepted: November 13, 2019
Article in press: November 13, 2019
Published online: January 26, 2020

P-Reviewer: Exbrayat JM, Grawish M, Sorio C, Liu X, Li SC
S-Editor: Zhang L
L-Editor: Filipodia
E-Editor: Xing YX

onto the surface of 10 μm thin *en face* tissue sections. No observable differences were seen in sphere migration, proliferation or differentiation in keratoconic tissue compared to normal between day 0 and D14. Spheres stained positively with Calcein-AM up to D14. Cell migration increased from day 0 to D14, occurring radially in three dimensions from the sphere and in alignment with tissue edges. Cell proliferation marker, EdU, was detected at day 10. Implanted spheres stained positively for putative stem cell markers ΔNp63α and ABCB5, while ABCG2, ABCB5, ΔNp63 and p63α were detectable by droplet digital PCR up to D14. Double immunolabelling revealed absence of ABCB5 staining in migrated cells but positive staining of alpha smooth muscle actin (myofibroblast marker) in some migrated cells. Droplet digital PCR showed similar expression patterns of differentiation markers but a reduction in stem cell markers between normal and keratoconic tissue with an increase in stromal cell markers and a reduction in epithelial cell markers, indicating an appropriate response to repopulating diseased tissue.

CONCLUSION
Cells from implanted stem cell-enriched spheres can repopulate a keratoconic corneal stromal surface in a directed manner and exhibit migratory stromal cell phenotypes.

Key words: Keratoconus; Cell culture; Immunohistochemistry; Quantitative PCR; Digital PCR; Spheroid; Holoclone; Neurosphere; Regeneration

Core tip: Keratoconus is a degenerative corneal disease characterised by aberrant cell behaviour and loss of matrix that can result in vision loss. Cells extracted from peripheral corneas can form stem cell-enriched spheres, which we introduced into normal and keratoconic corneal stroma. This study shows for the first time that implanted stem cell-enriched spheres are capable of repopulating the dystrophic corneal stromal surface in a directed manner. Spheres may therefore be used to replace or supplement diseased cells in keratoconic patients, thereby serving as an adjunct to current treatments.

Citation: Wadhwa H, Ismail S, McGhee JJ, Van der Werf B, Sherwin T. Sphere-forming corneal cells repopulate dystrophic keratoconic stroma: Implications for potential therapy. *World J Stem Cells* 2020; 12(1): 35-54
URL: https://www.wjgnet.com/1948-0210/full/v12/i1/35.htm
DOI: https://dx.doi.org/10.4252/wjsc.v12.i1.35

INTRODUCTION

Keratoconus is a degenerative ocular disease in which corneas of affected individuals become thin and protrude, resulting in the typical cone-shaped corneal distortion[1]. In keratoconus, the normal architecture and cell milieu of the anterior cornea is disrupted. Pathological changes include altered cell morphology, altered cell alignment and organisation, loss of resident keratocyte cell density from the corneal stroma, loss of cell matrix and eventually increased areas of fibrosis and scarring[2-6]. Both the epithelial and stromal layers of the cornea are affected but due to the complexity of this disease, it is still not definitively known in which layer/s the pathology originates[7]. Despite this, therapies like corneal collagen cross-linking[8,9], corneal transplantation (penetrating keratoplasty) and deep anterior lamellar keratoplasty that target the corneal stroma for treatment are efficacious.

Both corneal transplantation and corneal collagen cross-linking strengthen the central corneal stroma, and yet rates of disease recurrence are significantly less in transplanted patients despite having more advanced disease. Kelly *et al*[10] conducted a large cohort study in which they found 89% of grafts for keratoconus remained viable at 10 years, and only 4% of all regrafts were performed for recurrence. While some may argue that these cases of recurrence represent undiagnosed keratoconus in the

donor tissue[11], the rates of recurrence are significantly low even if these are a true recurrence in grafted tissues. After a cross-linking procedure, on the other hand, measures that may indicate disease recurrence, like simulated maximum keratometry values, increase as early as 18 mo after the procedure[12]. We hypothesise that decreased rates of recurrence in corneal transplant patients are due to the introduction of normal cells along with their normal matrix rather than simply removing the native aberrant cells in the central cornea. On a cellular level, both treatments remove the host's central epithelial cells and central keratocytes, the latter from either ultraviolet radiation-induced cell death during cross-linking and the former by removal entirely during transplantation. The host's limbal cells are preserved with both treatment modalities, which likely mount a wound healing response to repopulate the decellularised tissues. Within 6 mo, native keratocytes eventually repopulate the cross-linked native keratoconic stroma[13] and likely the transplanted corneal stroma also. Following this line of thinking, it may further be postulated that introducing healthy cells, into a keratoconic cornea, as a supplement to collagen cross linking, could perhaps impact the host cells and shift the balance from a degenerative state to a healthy state.

Stem cells are increasingly being studied for their potential use in regeneration and repair of tissues in many specialties and could be a promising potential method of introducing a sustainable source of normal cells into the keratoconic environment. Humans have an endogenous population of oligopotent adult stem cells that are involved in the maintenance of the structure and function of the cornea. The epithelial and stromal cell populations are maintained by corneal epithelial and stromal stem cells respectively. These stem cells reside in the corneal limbus, the area between the white sclera and transparent cornea, which make them relatively easily accessible to harvest. Corneal limbal stem cells can be extracted and isolated using the established neurosphere assay[14-16]. Corneal stem cell spheres are of mesenchymal origin. Numerous studies have demonstrated the ability of mesenchymal stem cells to enhance endogenous tissue repair by reducing inflammation and immune response, inducing angiogenesis, reducing apoptosis and oxidative stress and stimulating recruitment, retention, proliferation and differentiation of tissue-residing stem cells[17,18] and possibly through mitochondrial transfer[19]. Many of these reparative processes are impaired in keratoconus[20-25], which strengthens the case to evaluate the therapeutic potential of corneal stromal stem cell-containing spheres for keratoconus. Damaged rat corneas treated with mesenchymal stem cells have been shown to be able to restore visual function, probably by reducing levels of inflammatory markers interleukin-2, matrix metalloproteinase-2 and common leukocyte antigen and without differentiating into epithelial cells[26]. Looking at mesenchymal stem cells from the limbus in particular, human (and rabbit) limbal mesenchymal stem cells co-cultured with immune cells from mismatched donors *in vitro* have suppressed T cell proliferation by up to 75%[27], mediated by secretion of transforming growth factor beta-1[14]. The inherent immunosuppressant effect is important to note because keratoconus affects both eyes albeit asymmetrically. Therefore, autologous stem cells from the less affected eye are still likely to be affected by the dystrophic process.

Our laboratory and others have previously characterised stem cell-enriched spheres, which contain cells from a spectrum of less to more differentiated cells: Stem cells, transient amplifying cells and differentiated cells from a combination of epithelial and stromal origins[16,28]. We have also shown that spheres are dynamic entities that can maintain themselves for up to 4 mo[16], are capable of eliciting wound healing responses[29] and are capable of repopulating the normal stromal ocular surface[30]. To date, *in situ* stem cell sphere behaviours in response to diseased human corneal tissues have not been investigated. In this paper, we present our novel findings of the *in situ* behaviours of corneal stem cell spheres in response to dystrophic keratoconic stromal matrix.

MATERIALS AND METHODS

Human tissue

Fresh or frozen human central cornea, peripheral corneo-scleral tissue or whole corneo-scleral tissue from living or cadaveric donors were used with consent and handled in accordance with procedures approved by the Northern X Regional Ethics Committee and since reviewed by the Northern A Regional Ethics Committee (Ethics reference: NTX/07/08/080/AM06).

Sphere formation and culture

Corneo-limbal stromal tissues from cadaveric human donors were enzymatically

digested, the extracted cells mechanically filtered and then cultured in non-adherent conditions using Supplemented Neurobasal-A medium (standard culture medium) using the previously published method[16,30]. Cells congregated together and formed self-renewing, stem cell-enriched spheres. All spheres were maintained in culture for at least 21 d prior to use in implantation experiments. Medium changes (50% of the volume) were performed twice a week.

Preparation of tissue for sphere implantation

Four keratoconic central corneas from patients who were recipients of full-thickness penetrating keratoplasties (keratoconic button) and four central corneas from cadaveric donor corneas (non-keratoconic button) used for Descemet stripping automated endothelial keratoplasty (n = 2), Descemet's layer endothelial keratoplasty (n = 1) or decompensated cornea (tissue that failed New Zealand Eye Bank's endothelial count criteria for use as a graft, n = 1) were used for sphere implantation. Corneas from six donors were used for full thickness implants and corneas from four donors were used for creating tissue sections for implantation; corneas from two of these donors were used for both purposes.

Central corneal buttons: Corneal buttons were first decellularised by subjecting the tissue to three "freeze-thaw cycles," which has previously been shown to completely remove live cells[30]. Corneal buttons were then prepared for implantation as described in detail previously[31]. Briefly, the epithelium is scraped and rinsed away, v-shaped wedge incisions in the anterior two-thirds of the corneal buttons are created and then spheres are implanted within the incisions. Because de-epithelialized anterior stroma was used from each of keratoconic and non-keratoconic corneal buttons, tissues were deemed equivalent and comparable.

Implanted spheres were incubated at 37 °C for 10 min to encourage adherence to the tissue prior to addition of 2-3 mL of standard culture medium. The point at which spheres were able to be visualised *in situ* after culture medium had been added was defined as time equals day 0. Sphere-implanted tissues were inverted so that the epithelial side apposed the bottom of the Petri dish during culture and incubated at 37 °C for up to 10 d.

***En face* stromal sections:** Due to the limited availability of keratoconic tissue for research, it was pertinent to develop a method to maximise the use of available tissue. To facilitate this, we developed a technique for the placement of spheres onto e*n face* (coronal) 10 μm sections of central corneal tissue. Decellularised tissues were frozen at -20 °C in Tissue-Tek® OCT™ compound (OCT) (4583, Sakura) and cryosectioned to yield 10 μm thin tissue sections, which were washed thrice with sterile PBS for 10 min each to remove surrounding OCT prior to use. *En face* tissue sections were stored in PBS at 4 °C until required. One sphere was carefully seeded onto the surface of each 10 μm tissue section under a Leica DM IL inverted contrasting microscope, allowed to adhere and overlaid with culture medium as described above. Tissue sections from two keratoconic and two normal corneal "tissue donors" were seeded with a combination of spheres derived from six human donors (sphere donors).

Sphere-implanted tissues were cultured for up to 14 d and 50% medium changes were completed biweekly. At day 0, 1 and 3 or 4 post-seeding, sections were fixed for immunohistochemistry as described below. The rationale for these time points was based primarily on observations with spheres placed on collagen-coated surfaces, which indicated that these times were the critical points where an increase in cell migration and proliferation occurred. Experiments were concluded at day 14 due to the observation of complete tissue matrix repopulation.

Visualising live cells and proliferating cells

Live cells both within spheres and migrating outward were visualised using the LIVE/DEAD® Viability/Cytotoxicity Kit (L3224, Life Technologies), whereby samples were incubated in 2 μM Calcein-AM and 4 μM Ethidium homodimer-1 for 40 min at 37 °C. Staining solutions were then carefully aspirated, discarded and replaced with fresh culture medium.

Cell proliferation was detected using Click-iT® EdU Alexa Fluor® 594 Imaging Kit (C10339, ThermoFisher) by supplementing standard culture medium with 5-ethynyl-2′-deoxyuridine, a nucleoside analogue of thymidine, at a concentration of 10 μM.

Phase contrast, bright-field and fluorescence microscopy images were assessed and captured using the following microscopes: Leica DM-RA upright fluorescence microscope (Leica)–images analysed using NIS-Elements Basic Research Microscope Imaging Software version 4.30.00, Nikon TE2000 Inverted Fluorescence Microscope (Nikon)–images analysed using NIS-Elements Advanced Research Microscope Imaging Software version 4.50.00. and FLoid Cell Imaging station (Life Technologies).

Images were analysed using its fully integrated image capture and analysis system.

Immunohistochemistry

Immunohistochemistry was performed essentially as described previously[30]. Samples were fixed using 4% paraformaldehyde (Sigma) unless specified otherwise, permeabilised with ice cold methanol for 20 min to expose antigens, blocked with a solution of 100 mM glycine, 0.1% Triton X-100 and 10% normal goat serum (NGS) to reduce non-specific binding of subsequent antibody treatments, incubated with primary antibodies overnight at 4 °C, secondary antibodies for 3 h and the nuclear stain DAPI (D9542, Sigma). Samples were immersed in Citifluor anti-fade reagent and sealed with a coverslip for viewing with fluorescence microscopy.

Primary antibodies used in this work were as follows: Anti-ATP binding cassette subfamily B member 5 (anti-ABCB5) antibody produced in rabbit at 1:125 (HPA026975, Sigma), anti-tumour protein p63 alpha chain, N-terminal isoform (anti-ΔNp63α) antibody produced in rabbit at 1:160 (private order, PickCell Laboratories) and anti-smooth muscle actin (anti-αSMA) antibody produced in mouse at 1:80 (A2547; Sigma Aldrich). Secondary antibodies were used at 1:350 goat anti-mouse Alexa488 (A11029, ThermoFisher) to detect anti-αSMA, goat anti-rabbit Alexa488 (A11034, ThermoFisher) to detect anti-ΔNp63α and goat anti-rabbit Alexa568 (A11011, ThermoFisher) to detect anti-ABCB5 primary antibodies.

Based on previously established methodologies[16,30], an adapted protocol was used for cross-sections of implanted full-thickness tissues. Sphere-implanted corneal buttons were frozen at -20 °C in Tissue-Tek® OCT compound (Sakura) before being cryosectioned to obtain 20 μm "cross-sections," which were mounted onto glass microscope slides. These cross-sections were washed in PBS for 10 min three times. Sections were fixed with 2.5% paraformaldehyde in PBS for 10 min (except those for detecting ΔNp63α, which were not fixed) and rinsed in PBS for 15 min three times. Sections were treated with 2 mg/mL bovine testicular hyaluronidase in PBS for 1 hour at 37 °C in a humidity chamber, permeabilised in methanol at -20°C for 20 min and washed in PBS for 15 min three times. This was followed by treatment with 20 mM glycine in PBS for 30 min at room temperature and washed in 0.1% NGS in PBS three times for 15 min. Sections were subsequently treated with a 2% NGS with 0.1% Triton X-100 in PBS solution for 30 min at room temperature. Primary and secondary antibodies were prepared in 0.1% NGS to desired concentrations as described earlier and sections incubated overnight in primary antibody prior to washing with 0.1% NGS and incubation in secondary antibody for 2 h at ambient temperature. Counterstaining was completed with 0.1 μg/mL DAPI for 10 min prior to mounting in Citifluor antifade using a glass coverslip, which was sealed with nail varnish. The microscopes and imaging software used were: The Leica DM-RA upright fluorescence microscope described earlier and the Olympus FV 1000 Confocal laser scanning microscope (Olympus) with the FV10-ASW ver.0.4.00 image capture and analysis software.

Gene expression quantification

Sphere implanted tissue sections were carefully removed from the glass slide and transferred to an RNase-free tube. RNA extraction and genomic DNA removal was subsequently performed using the $_{RNA}$Gem™ Tissue Plus Kit (RTP0200, ZyGem) as per manufacturer's protocol. Samples were tested for presence of PCR inhibitors using the SPUD assay[32]. Inhibitory samples were further purified using the PureLink® RNA Mini Kit (12183018A, ThermoFisher) as per manufacturer guidelines as required. Complementary DNA (cDNA) was synthesised using the SuperScript® VILO™ cDNA Synthesis Kit (11754-050, ThermoFisher) according to manufacturer guidelines using 10 μL of the DNase I treated total RNA extracts.

Successful cDNA synthesis was confirmed by performing a β-actin polymerase chain reaction on all cDNA preparations and resolving PCR products by agarose gel electrophoresis to confirm successful amplification. The following primers were used: AACTCCATCATGAAGTGTGACG (forward) and GATCCACATCTGCTGGAAG (reverse) which yield a 224 bp amplicon. cDNA samples were subsequently diluted 1:5 and then analysed using droplet digital PCR (ddPCR). The primers and probes used are listed in Table 1. All primers were commercial PrimeTime qPCR assays that utilise the 56-FAM fluorophore and both the ZEN and 3IABkFQ quenchers. Detailed sequences of the primer set and probe sequences can be obtained from the manufacturer.

For each ddPCR assay, one positive control and one "no template" control was included in addition to samples. Purified PCR product used at a concentration of 1.2 × 10^4 copies/μL were used for the positive controls.

PCR reactions were set up containing final concentrations of 1 × PrimeTime qPCR assay, 1 × ddPCR supermix for probes (no dUTP) and 2 μL of diluted cDNA in 24 μL

Table 1 PrimeTime quantitative polymerase chain reaction assays used for droplet digital polymerase chain reaction

Product of interest: Gene	Reference gene or gene of interest	Assay identification	Size of complimentary DNA amplicon, base pairs
Actin, beta	Reference	Hs.PT.39a.22214847	109
Beta-2-microglobulin	Reference	Hs.PT.58v.18759587	142
Glucuronidase beta	Reference	Hs.PT.58v.27737538	127
Glycreraldehyde-3-phosphate dehydrogenase	Reference	Hs.PT.39a.22214836	142
Hypoxanthine phosphoribosyltransferase 1	Reference	Hs.PT.58v.45621572	148
Peptidylprolyl isomerase A	Reference	Hs.PT.58v.38887593. g	101
Actin, alpha 2, smooth muscle, aorta	Gene of interest	Hs.PT.56a.2542642	131
ATP binding cassette subfamily B member 5	Gene of interest	Hs.PT.58.38502346	106
ATP-binding cassette, sub-family G member 2	Gene of interest	Hs.PT.58.20889058	114
Collagen type I, alpha 1 chain	Gene of interest	Hs.PT.58.15517795	130
Collagen type I, alpha 2 chain	Gene of interest	Hs.PT.58.26714160	108
Integrin, subunit beta 1	Gene of interest	Hs.PT.58.39883300	141
Keratin 3	Gene of interest	Hs.PT.58.25330614	126
Keratocan	Gene of interest	Hs.PT.58.45594658	130
Laminin, subunit alpha 1	Gene of interest	Hs.PT.58.3170022	129
Notch1	Gene of interest	Hs.PT.58.23074795	112
Proliferating cell nuclear antigen	Gene of interest	Hs.PT.58.4761611	94
Tumour protein p63, transcript variant 1, C-terminal isoform α	Gene of interest	Hs.PT.58.39019253	108
Tumour protein p63, transcript variant 1, N-terminal isoform	Gene of interest	Hs.PT.58.19710922	104
Vimentin	Gene of interest	Hs.PT.58.38906895	141

reactions. Where samples did not yield an expression quantity due to low target abundance, increasing amounts of diluted cDNA from 2 μL, 4 μL, 6 μL up to a maximum of 10 μL were used in repeat reactions. For droplet generation, 20 μL of each PCR reaction was loaded into the appropriate wells of DG8 droplet generation cartridges along with 70 μL of droplet generation oil, covered with a DG8 gasket and placed into the droplet generator to generate droplets. Droplets (40 μL) were transferred to a semi-skirted PCR plate, sealed and amplified in a C1000 Touch thermal cycler (Bio-Rad). The thermal-cycling conditions used were: 95 °C for 10 min for initialisation followed by 40 cycles of denaturation at 94 °C for 30 s and annealing at 60 °C for 60 s. After cycle 40, samples were heated to 98 °C for 10 min and cooled to 12 °C for temporary storage. After amplification, fluorescent and non-fluorescent droplets were analysed using the Bio-Rad QX200 droplet reader (Bio-Rad). The resulting ddPCR data was analysed with QuantaSoft analysis software (version 1.7.4). A threshold line was manually placed above the negative level determined from the no template control and below the positive level determined from the positive control.

Results were normalised to the geometric mean of six reference genes (listed in Table 1). Expression difference in spheres implanted on *en face* keratoconic tissue sections and cultured over 14 d were compared to freshly implanted spheres at day 0 (calibrator sample).

Biostatistics

Statistical analysis on normalised gene expression values generated by ddPCR was conducted with a linear mixed model having donor and day within donor as random terms. Fixed model terms were gene, diseased matrix and day. Data values were natural log transformed to meet the assumptions of the analysis. Calculations were done using the lme4 package[33] in R version 3.5.0[34]. The resulting estimates with their covariances were used to create the values in Table 2, Table 3 and Figure 1. The statistical methods of this study were reviewed by Bert Van der Werf, biostatistician from The University of Auckland.

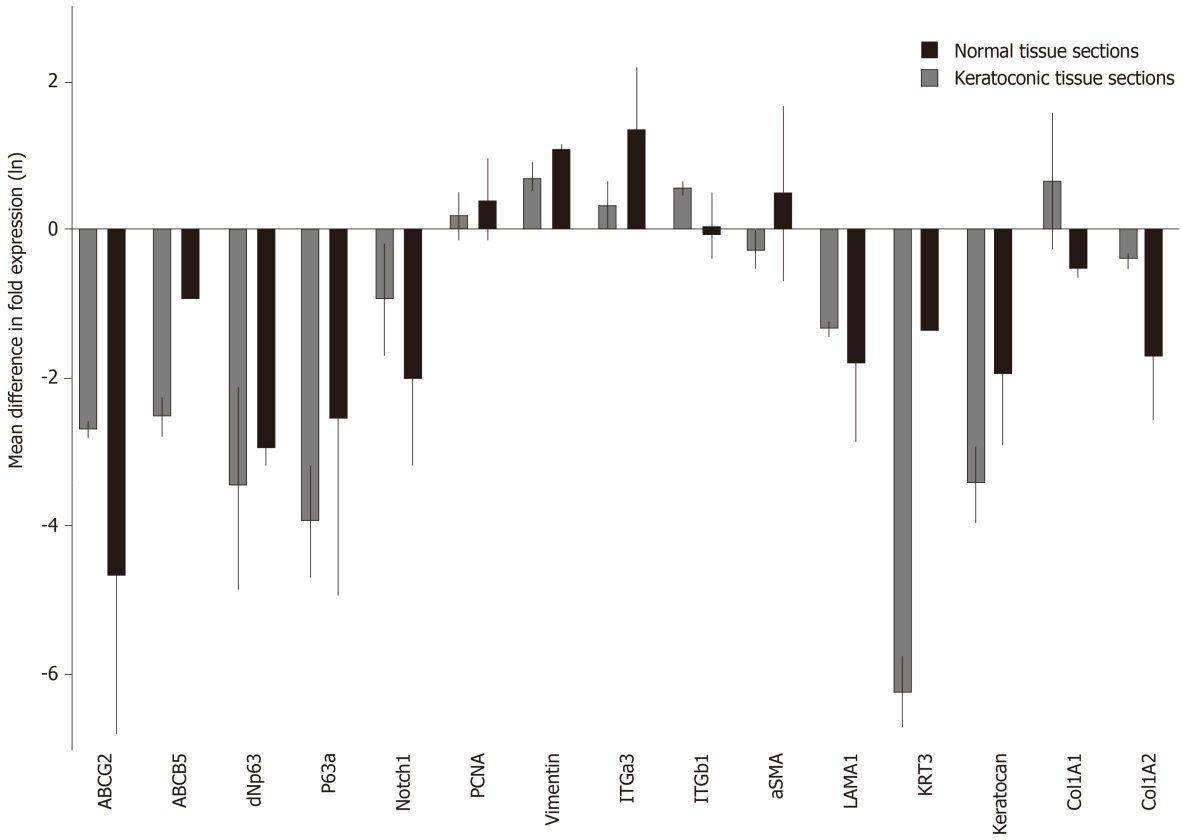

Figure 1 Estimated fold differences in expression of proliferation, stem cell and epithelial and stromal cell markers in sphere-seeded tissue sections at day 14. Expression of stem cell markers: ATP-binding cassette, sub-family G member 2, ATP binding cassette subfamily B member 5, tumour protein p63, transcript variant 1, N-terminal isoform, tumour protein p63, transcript variant 1, C-terminal isoform α, limbal niche marker Notch1, proliferation marker proliferating cell nuclear antigen, mesenchymal cell marker vimentin, adhesion molecules integrin subunit α3 and β1, myofibroblast marker alpha smooth muscle actin, epithelial markers laminin α1 and keratin 3, keratocyte marker keratocan, collagen type I, alpha 1 chain and collagen type I, alpha 2 chain genes in sphere-seeded normal and keratoconic 10 μm *en face* decellularised central corneal stromal tissue sections. Spheres were derived from two human donors and expression data at days 0 and 14, normalised to reference genes β-actin, glycreraldehyde-3-phosphate dehydrogenase, glucuronidase beta, hypoxanthine phosphoribosyltransferase 1, peptidylprolyl isomerase A and β2-microglobulin. Data is expressed as estimated fold difference between day 14 and day 0 based on raw data and plotted as the natural logarithm mean differences in fold expression ± standard deviation.

RESULTS

Repopulation of keratoconic tissue surface

Spheres were seeded on to a total of 28 thin 10 μm tissue sections and assessed for viability. Cells were deemed non-viable based on complete absence of LIVE staining of cells across the entire implanted tissue section. Of these 28 tissue sections, 17 were keratoconic tissue sections and 11 were normal tissue sections. The keratoconic and normal tissue sections were each sourced from two different human tissue donors. Cells were viable in 28 out of 28 (100%) tissue sections assessed at day 1 post-seeding. Two tissue sections were fixed for immunohistochemistry. The remaining 26 tissue sections (16 keratoconic and 10 normal) were assessed at day 3, of which 20 (77%) were viable. Six tissue sections, two keratoconic and four normal, were non-viable, and two tissue sections were fixed for immunohistochemistry. At day 7, 18 tissue sections were assessed with the viability stain, of which 16 (89%) were viable. Spheres and cells remained viable at day 14 in at least two keratoconic tissue sections. All of the tissue sections that became non-viable were implanted with spheres from the same donor. However, two other keratoconic and two other normal tissue sections implanted with spheres derived from this sphere donor remained viable to day 7 (Table 4).

Viable cells increased in number and migrated over observed time periods between 0 and 14 d. Cells were seen to have migrated radially in all directions from the centre of spheres as early as day 1. Similar processes were observed in keratoconic and normal tissues. Sphere-derived cells completely repopulated the surfaces of keratoconic tissue sections (Figure 2A) (n = 2) at day 14 (Figure 2B). Cells at tissue edges at various time points were observed to align with the edge (example in Figure 3A, white arrows). Migrated cells were not seen on the culture dish surface in any

Table 2 Statistical analysis of difference in gene expression in sphere-seeded tissue sections as measured by droplet digital polymerase chain reaction, effect of time: day 0 *vs* day 14

	Day 0	Day 14	Day 14 - Day 0	
Target	Estimate[1] (lower.95, upper.95)	Estimate[1] (lower.95, upper.95)	*P*	
ABCB5	0.02 (0.01, 0.08)	0 (0, 0.01)	0.003	S
ABCG2	0.71 (0.25, 1.99)	0.02 (0.01, 0.05)	0.000	S
aSMA	0.21 (0.07, 0.58)	0.23 (0.09, 0.62)	0.871	NS
Col1A1	4.66 (1.65, 13.12)	4.97 (1.84, 13.44)	0.929	NS
Col1A2	11.33 (4.02, 31.92)	3.89 (1.44, 10.52)	0.145	NS
dNp63	0.03 (0.01, 0.09)	0 (0, 0)	0.000	S
ITGa3	0.12 (0.04, 0.33)	0.28 (0.10, 0.75)	0.244	NS
ITGb1	5.81 (2.06, 16.36)	7.99 (2.96, 21.59)	0.663	NS
Keratocan	0.14 (0.05, 0.39)	0.01 (0, 0.03)	0.000	S
KRT3	0.28 (0.08, 0.96)	0 (0, 0.01)	0.000	S
LAMA1	0.33 (0.12, 0.94)	0.07 (0.03, 0.19)	0.032	S
Notch1	0.43 (0.15, 1.21)	0.10 (0.04, 0.26)	0.043	S
P63a	0.05 (0.02, 0.15)	0 (0, 0.01)	0.000	S
PCNA	0.52 (0.19, 1.48)	0.71 (0.26, 1.92)	0.681	NS
Vimentin	16.96 (6.02, 47.77)	42.18 (15.61, 113.96)	0.214	NS

[1]Values are the back-transformed estimates from the multivariate regression; NS: Not significant; S: Significant ($P \leq 0.05$); ABCB5: ATP binding cassette subfamily B member 5; ABCG2: ATP-binding cassette, sub-family G member 2; αSMA: Smooth muscle, actin; COL1A1: Collagen type I, alpha 1 chain; COL1A2: Collagen type I, alpha 2 chain; TP63: Tumour protein p63; ΔNP63: Transcript variant 1, ΔNP63: N-terminal isoform, ITGa3: Integrin, subunit alpha 3; ITGB1: Integrin, subunit beta 1; KRT3: Keratin 3; LAMA1: Laminin, subunit alpha 1; TP63: Tumour protein p63; PCNA: Proliferating cell nuclear antigen.

samples where tissue sections had not been completely repopulated. Two tissue sections, both keratoconic, were observed to be repopulated to complete confluency. Periodic examination of these two samples with a light microscope revealed that at approximately day 11, cells appeared to migrate initially as cell columns when leaving the tissue edge (although not invariably), and then cells would migrate to fill the space between the columns. Cells at the leading edge of these migratory columns had fine cell processes connecting the cells to neighbouring cells (Figure 3B, orange arrows).

Immunohistochemistry of sphere-seeded tissue sections

Spheres seeded onto keratoconic tissue sections stained positively for the putative stem cell marker ABCB5 and the myofibroblast marker αSMA at day 0, day 1 and day 4. At all three time points, labelling of ABCB5 appeared to be concentrated within spheres and not outside (Figure 4A-C, red), indicating presence of stem cells within spheres alone. Appearance of positive αSMA staining in small numbers of cells within spheres (Figure 4A-C, green) indicated some differentiation to myofibroblast cells (highly likely from daughter cells), and indeed some of these αSMA-positive cells were seen outside spheres at day 1 (Figure 4D) but also at day 4. Positive staining was above the fluorescence signal of the secondary antibody only control (Figure 4E).

Gene expression analysis

Analysis of variance revealed a significant effect of day (day 0 *vs* day 14; $P \leq 0.016$) and diseased matrix (keratoconic *vs* normal; $P \leq 0.006$). At day 14 post sphere seeding, there was an overall significant reduction in expression of putative stem cell makers (ABCB5, ATP-binding cassette, sub-family G member 2 (ABCG2), ΔNp63, tumour protein p63 C-terminal isoform α (p63α)), limbal (notch1), epithelial (keratin 3), keratocyte (keratocan) and extracellular matrix (laminin α1 (LAMA1)) markers tested using ddPCR (Table 2; Figure 1). In both keratoconic and normal tissue sections, expression of the putative stem cell markers and the limbal niche marker notch1 decreased over time as did the epithelial and extracellular matrix markers keratin 3, collagenA2, laminin and the stromal cell marker keratocan. While proliferating cell nuclear antigen (PCNA), vimentin and the adhesion molecules integrin alpha 3 and integrin beta 1 all increased at day 14 in both keratoconic and normal tissue matrices

Table 3 Statistical analysis of difference in gene expression in sphere-seeded tissue sections as measured by droplet digital polymerase chain reaction, effect of matrix, keratoconic *vs* normal

	Keratoconic	Normal	Keratoconic-normal	
Target	Estimate[1] (lower.95, upper.95)	Estimate[1] (lower.95, upper.95)	*P*	
ABCB5	0 (0, 0.01)	0.01 (0, 0.03)	0.351	NS
ABCG2	0.03 (0.01, 0.09)	0.37 (0.14, 0.99)	0.001	S
aSMA	0.24 (0.09, 0.64)	0.20 (0.07, 0.54)	0.800	NS
Col1A1	6.40 (2.37, 17.25)	3.62 (1.34, 9.77)	0.418	NS
Col1A2	9.30 (3.45, 25.08)	4.74 (1.76, 12.79)	0.337	NS
dNp63	0 (0, 0.01)	0.02 (0.01, 0.05)	0.004	S
ITGa3	0.16 (0.06, 0.43)	0.21 (0.08, 0.56)	0.695	NS
ITGb1	7.63 (2.83, 20.57)	6.09 (2.26, 16.42)	0.748	NS
Keratocan	0.03 (0.01, 0.08)	0.04 (0.02, 0.12)	0.588	NS
KRT3	0.01 (0.01, 0.04)	0.04 (0.01, 0.12)	0.211	NS
LAMA1	0.17 (0.06, 0.46)	0.13 (0.05, 0.36)	0.726	NS
Notch1	0.07 (0.03, 0.20)	0.58 (0.21, 1.56)	0.003	S
P63a	0.01 (0, 0.01)	0.02 (0.01, 0.06)	0.053	NS
PCNA	0.51 (0.19, 1.38)	0.73 (0.27, 1.97)	0.612	NS
Vimentin	24.29 (9.01, 65.52)	29.45 (10.92, 79.43)	0.784	NS
ABCB5	0 (0, 0.01)	0.01 (0, 0.03)	0.351	NS

[1]Values are the back-transformed estimates from the multivariate regression; NS: Not significant; S: Significant ($P \leq 0.05$); ABCB5: ATP binding cassette subfamily B member 5; ABCG2: ATP-binding cassette, sub-family G member 2; αSMA: Smooth muscle, actin; COL1A1: Collagen type I, alpha 1 chain; COL1A2: Collagen type I, alpha 2 chain; TP63: Tumour protein p63; ΔNP63: Transcript variant 1, ΔNP63: N-terminal isoform, ITGa3: Integrin, subunit alpha 3; ITGB1: Integrin, subunit beta 1; KRT3: Keratin 3; LAMA1: Laminin, subunit alpha 1; TP63: Tumour protein p63; PCNA: Proliferating cell nuclear antigen.

(Figure 1).

When comparing tissue matrices (keratoconic *vs* normal sections), there were no significant differences in gene expression between spheres seeded on keratoconic tissue sections and spheres seeded on normal tissue sections for cell proliferation (PCNA), epithelial (keratin 3), keratocyte (keratocan), extracellular matrix (LAMA1), collagen I α1 (Col1A1), collagen I α2 (Col1A2)), adhesion (integrin α3, integrin β1), myofibroblast (αSMA) or mesenchymal cell (vimentin) markers tested using ddPCR (Table 3; Figure 1). Only limbal and stem cell markers (notch1, ABCG2, ΔNp63) showed a significant reduction in gene expression on keratoconic sections, while p63α reduced to a level that did not reach significance ($P = 0.053$). The putative stem cell marker ABCB5 was also observed to have reduced expression on keratoconic matrix but not significantly so (Table 3; Figure 1).

Only the repair cell marker αSMA showed an overall increase in normal tissue sections and a decrease in keratoconic tissue sections, while conversely collagenA1 showed a decrease in normal tissue sections and an increase in keratoconic tissue sections (Figure 1). However, this difference in expression pattern on normal *versus* diseased tissue matrix was not statistically significant, which may be due to sphere donor variation for both αSMA and collagenA1.

Sphere implantation into full thickness tissue

Sphere behaviours once implanted into full thickness keratoconic tissue were similar to those observed on thin tissue sections and to those observed in full thickness non-keratoconic tissue controls. Six decellularised full-thickness central corneal tissues (corneal buttons) from post-keratoplasty keratoconic patients ($n = 3$) and from non-keratoconic cadaveric donor corneas with normal anterior corneas ($n = 3$) were successfully implanted with a total of 16 spheres using our wedge-shaped incision technique. The spheres were derived from three different human donors: Eight implanted in keratoconic tissue and eight implanted in non-keratoconic tissue. All spheres successfully survived the implantation procedure (confirmed by positive staining with Calcein-AM), tissue handling and new culture conditions for at least three days from the time of implantation (day 3) as seen in Figure 5A-B. In implanted keratoconic buttons, six of eight spheres and their derivative cells were viable at day

Table 4 Viability of spheres cultured on keratoconic and normal tissue sections

Day post implantation	Keratoconic tissue sections		Normal tissue sections	
	Number of sphere-implanted tissue sections cultured to time point	Number of sphere-implanted tissue sections viable at time point	Number of sphere-implanted tissue sections cultured to time point	Number of sphere-implanted tissue sections viable at time point
0	17		11	
1	17	17	11	11
3	16	14	10	6
7	13	11	5	5
14	2	2		

7. In comparison, five of eight spheres and their derivative cells were viable at day 7 in non-keratoconic buttons.

Cell migration was monitored to day 7 post-implantation in all implanted buttons with two buttons extended out to day 10 (Figure 5C-D). All implanted spheres exhibited radial cell migration from the centre of the sphere up to day 3, however the extent of cell migration from each sphere varied not only in replicate tissue samples but also within the same tissue. The extent of cell migration from the centre of spheres increased from day 3 to day 7 in 11/16 implanted spheres. Of the five spheres that did not increase cell migration from day 3 to day 7, two were implanted in keratoconic tissue and three in non-keratoconic tissue. An example of this is shown in Figure 5D where the sphere marked by a yellow arrow shows reduced cell migration at day 10 compared with day 3 (Figure 5B).

Cell morphology and cell orientation was variable in different areas of the implanted tissue. However, morphological patterns and cell orientation patterns in the keratoconic and non-keratoconic corneal buttons were similar. Cells close to the sphere (Figure 5E) were long and thin in appearance with their long axes appearing to radiate away from the centre of the sphere. The cells distant from the sphere appeared plumper (Figure 5F). The long axes of cells at the edge of the tissue appeared parallel to the edge, whereas the long axes of those distant from both the tissue edge and centre of spheres seemed to have no obvious pattern of alignment (Figure 5G). Cells that migrated from two spheres implanted close to one another seemed to align to form what appeared to be "cellular bridges" between the spheres (Figure 5C, white arrows).

The incisions made for implantation into the full-thickness tissue do not appear to significantly affect cell migration. Sphere-derived cells migrate to an incision, align with the incised tissue edge and over time the incision lines cannot be clearly demarcated and migrated cells can be seen on both sides of the incision. The left-most sphere in the implanted normal button in Figure 5B and 5D illustrates this.

Cross-sectional immunohistochemistry

Cross sections through implanted non-keratoconic and keratoconic corneal buttons were analysed by immunohistochemistry to further characterise the phenotypes of these cells. Cells within implanted spheres stained positively for the putative stem cell marker ΔNp63α while migrated cells did not (Figure 6A-B). Cells within implanted spheres as well as cells adjacent to but outside of the sphere (Figure 6C-D) stained positively for proliferation marker EdU at day 10.

DISCUSSION

Spheres derived from normal peripheral cornea behave normally on keratoconic matrix

Spheres and sphere-derived cells implanted in or on keratoconic tissue elicited similar viability, adherence, migration, division and differentiation responses to non-keratoconic tissue (normal anterior corneas). Spheres have previously been shown to be able to remain viable when implanted into normal peripheral corneal tissue matrix[30]. This study shows that spheres can also remain viable in central corneal tissue matrix. Notably for the first time, we have also shown that spheres can remain viable in diseased tissue matrix. Moreover, the spheres themselves maintained their morphological structure in most cases. The same implantation technique that we have previously employed for normal peripheral cornea was used for keratoconic central corneas. This shows that the implantation technique can be used with more friable

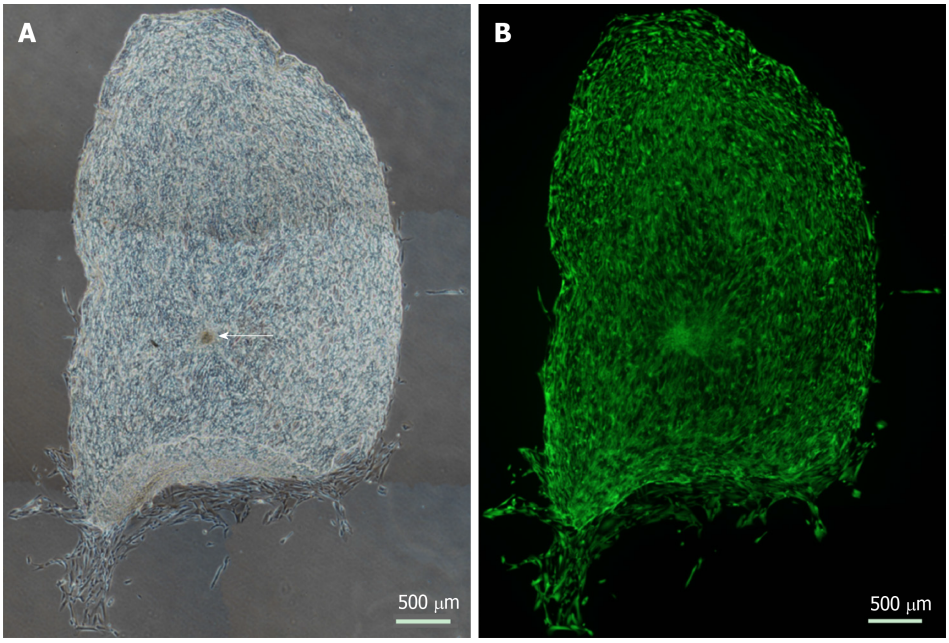

Figure 2 Cellular repopulation of the surface of *en face* keratoconic tissue sections. A: A stem cell-enriched sphere (arrow) was seeded onto a keratoconic decellularised central corneal stromal section (phase contrast image); B: Assessed for viability with Calcein-AM (green) at day 14 (fluorescence image). Montage imaging of the entire tissue section shows cells have repopulated the tissue section to complete confluence by day 14. Scale bar = 500 μm.

and weaker tissues as are apparent in severe keratoconus.

No observable difference was seen in viability between spheres implanted on keratoconic tissue and non-keratoconic tissue. Implanted tissues were cultured for up to 14 d, and spheres demonstrated the potential to remain viable for the entire duration. However, some spheres lost viability prematurely in some keratoconic and normal tissues even with biweekly medium changes. Speculative causes include intersphere variability or focal features of matrix that were not conducive to sphere growth (even in normal implants). The loss of sphere viability is unlikely to be attributable to matrix type (normal or diseased) as there was no consistency in terms of which matrix spheres prematurely lost viability. The initial implantation procedure, tissue handling or change in culture conditions are also unlikely causes as all spheres survived at least the first day. In our experience, spheres are discrete entities. The relative proportions of stem, progenitor, epithelial and stromal cells that comprise each sphere can vary. This intersphere variability may have been responsible for some spheres losing viability over time as the environment they were seeded/implanted into may not have supported the propagation of the majority cell populations present within these spheres.

There was no qualitative difference observed in the ability of spheres and their derivative cells to adhere to keratoconic tissue compared with normal tissue. Although the levels of relevant adhesion molecules in keratoconus used by nonimmunological migrating corneal cells are not known, decreased levels of collagen XII[35], integrin beta 4[36] and interfibrillar and interlamellar cohesive forces[37] have been observed in keratoconic stroma. However, these are unlikely to be applicable to the adhesion of spheres to stroma. The patterns of expression of integrin α3 and β1 chains, which dimerise to form the adhesion molecule integrin α3β1 found in basal epithelium and stromal cells, showed an increase at day 14 post-seeding of spheres, although this was not-significant ($P \leq 0.7$). Thus there was no clear pattern of expression differentiating normal *vs* keratoconic matrices in our ddPCR results.

Both the extent and pattern of cell migration observed in keratoconic tissues were similar to those observed in normal tissues. Cells tended to migrate from the sphere radially in all directions and this increased over time, as has been observed previously in peripheral corneo-scleral rims[30]. This is expected, given that there is no limbal or scleral region to polarise cell migration in a particular direction as is the case in peripheral cornea. Cells in keratoconic tissue appeared to respond to other nearby spheres as seen previously in normal tissue[16]. They also appeared to respond to the tissue edge, reflected by the apparent alignment of cells observed when implanted spheres were close to one another coupled with a consistent change in orientation when cells approached the tissue edge. These observations suggest that sphere-derived cells recognise tissue boundaries. In full thickness tissue, the tissue edge may

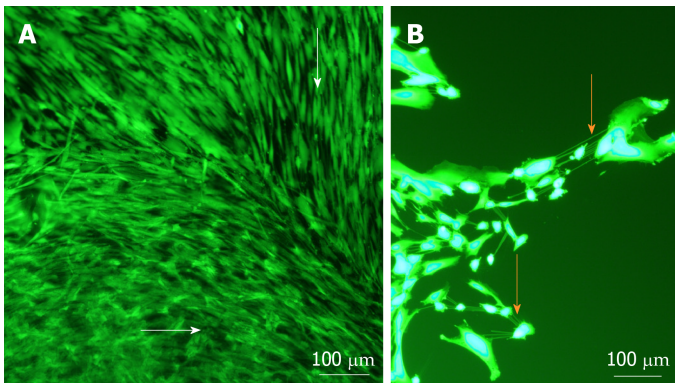

Figure 3 Cell morphology and migration patterns on the surface of sphere-seeded *en face* keratoconic tissue sections. A: Representative images of migrated cells over the surface of keratoconic tissue sections show cells from the centre of the sphere aligned radially while cells close to the tissue edge align parallel with the tissue edge (white arrows show cell orientations); B: When cells at one of the migrating edges are magnified and overexposed, fine cell projections can be seen connecting cells to neighbouring ones (orange arrows). Scale bar = 100 μm.

have provided a physical barrier. However, in tissue sections cells migrated beyond the tissue section boundaries and onto the dish surface eventually but not prior to complete repopulation of the stromal section. This is despite the dish being a tissue culture treated surface designed to promote cellular attachment and outgrowth. This confirms that the corneal collagen matrix is the preferred substrate for sphere-derived cells. Although our results show cell migration primarily on the surface of full thickness tissues, previous results with induced pluripotent cells have shown cells can also migrate deeply within tissue[38].

Our results assessing active cell division confirmed the presence of EdU within sphere cells and amongst migrating cells as well as continued expression of PCNA over time. PCNA expression showed variability between sphere donors suggesting the proliferative response was not temporally the same between donors. By 14 d, PCNA expression had increased from day 0 in all samples, which corresponds to the observation of complete tissue section repopulation at this time point.

Collectively, these results show that the abnormal structure of the diseased tissue was not a deterrent to sphere attachment, migration and division. However, there was no observable increase in any of these measures in response to diseased tissue compared to normal tissue either.

Functionality of the repopulated cells

Spheres, although stem cell enriched, do not exclusively contain undifferentiated cells[16,30]. Our findings were consistent with these cited observations. In addition, our findings also showed that spheres may maintain their stemness to some extent for at least 14 d after implantation in both keratoconic and normal implants. This was evidenced by their ability to maintain their definitive sphere structure *in situ*, detection of gene expression of putative stem cell markers over time and positive immunostaining of some of these markers (ΔNp63α and ABCB5). However, this retention of stemness was significantly reduced on keratoconic tissue sections (Table 3).

The reasons for this significant reduction in expression of stem cell markers on keratoconic matrix is unclear. It may be a tissue effect in that there is less signal coming from keratoconic tissue to maintain stem cells. Alternatively, it may be a cell effect in that stem cells within spheres change their response to diseased tissue more towards a pattern of differentiation rather than maintaining stemness. This may indicate that a greater number of spheres will be required to repair dystrophic tissue. Additionally, diseased tissue may be too far outside of the required stem cell niche to perpetuate maintenance of the stem cells to the same level as that of normal tissue. In our laboratory's previous results[30], we also observed a reduction in expression levels of putative stem cell markers to undetectable levels over time by qPCR. Presumably, this was due to the sheer numbers of migrated and differentiated cells over time diluting out the relatively few stem cells being maintained within a sphere. ddPCR is considered more sensitive than qPCR for detecting low abundance targets. Our ddPCR data in this study correlated well with previous qPCR data. ABCG2 expression decreased at similar rates in keratoconic implants and normal implants over 14 d. Similarly, stem cell markers ABCB5, ΔNp63 and p63α and limbal niche marker notch1 were detectable at low levels by ddPCR and also decreased by day 14.

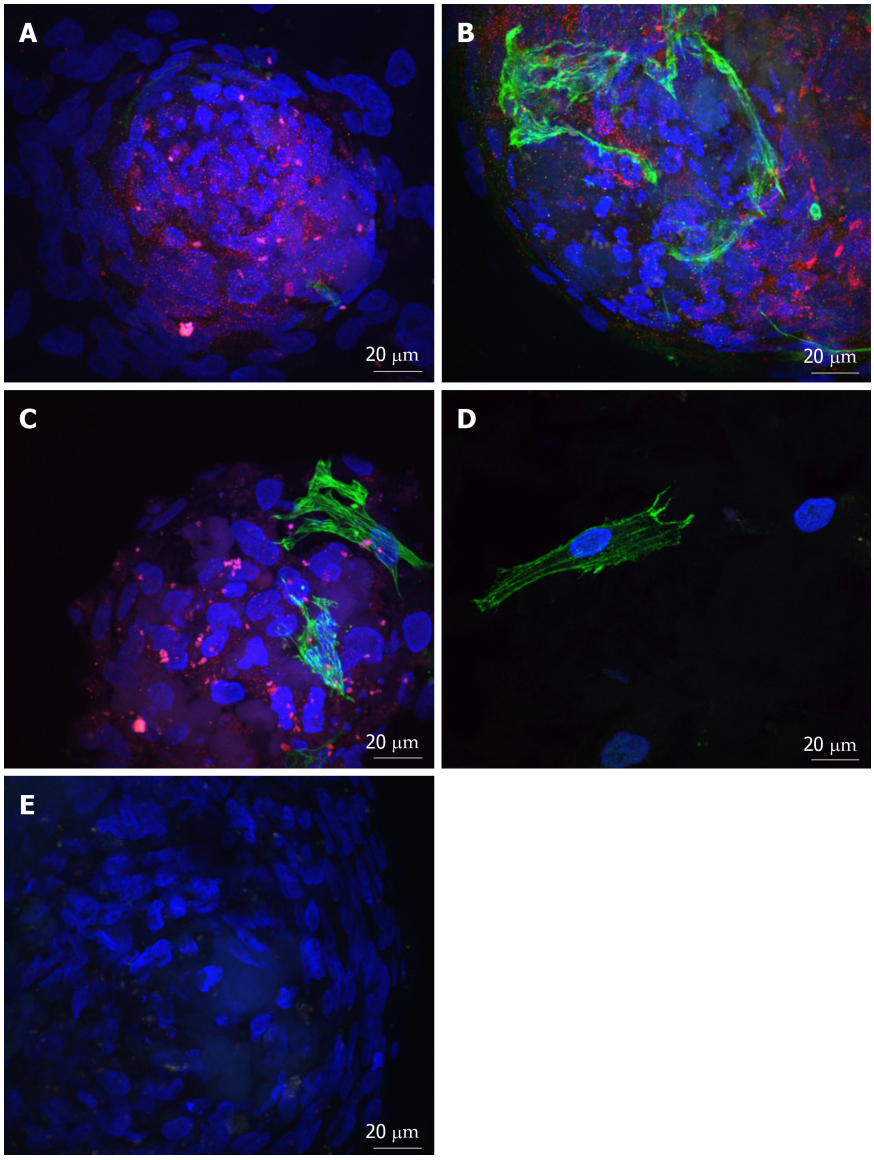

Figure 4 Adenosine triphosphate binding cassette subfamily B member 5 and α-smooth muscle actin expression in spheres and migrated cells seeded onto keratoconic tissue sections. A, B, C: Spheres seeded onto keratoconic tissue sections were fixed at day 0, 1 and 4 post-implantation and double primary antibody immunolabelled with putative stem cell marker ATP binding cassette subfamily B member 5 (ABCB5) (red) and myofibroblast marker alpha smooth muscle actin (αSMA) (green). Cell nuclei were counterstained with DAPI (blue). Confocal projection images of z stacks were taken. Spheres labelled positively with ABCB5 and αSMA at days 0 (A), 1 (B) and 4 (C); D: Migrated cells at days 1 and 4 appeared similar, a representative image at day 1 is shown; E: Spheres labelled with secondary antibody had no detectable red and green fluorescence when imaged at the same levels as A-C. Scale bar = 20 μm.

Our current findings reinforce our previous thoughts that message from differentiated cells was saturating any stem cell messages present from the few stem cells contributing to any given cDNA sample.

The evidence for cells differentiating as they leave the sphere lies in the absence of purported stem cell markers in migrated cells, cell morphologies of migrated cells and the presence of differentiation markers. Culture in serum-containing medium is known to stimulate differentiation, so this result is not surprising. Most cells that migrated from spheres at any time point between day 1 and 14 had a fusiform morphology. There was a noticeable effect at days 7 and 14 on the cell migration patterns of spheres placed on to keratoconic stromal sections that appeared to have a much looser arrangement of collagen fibrils. In these sections, cell orientation took on a less organized and a more random orientation pattern that was not observed in normal stromal sections. Coupled with an observed increase in expression of mesenchymal marker vimentin over time when compared to day 0, there is a good chance that these cells were stromal fibroblasts, which may or may not have been activated fibroblasts.

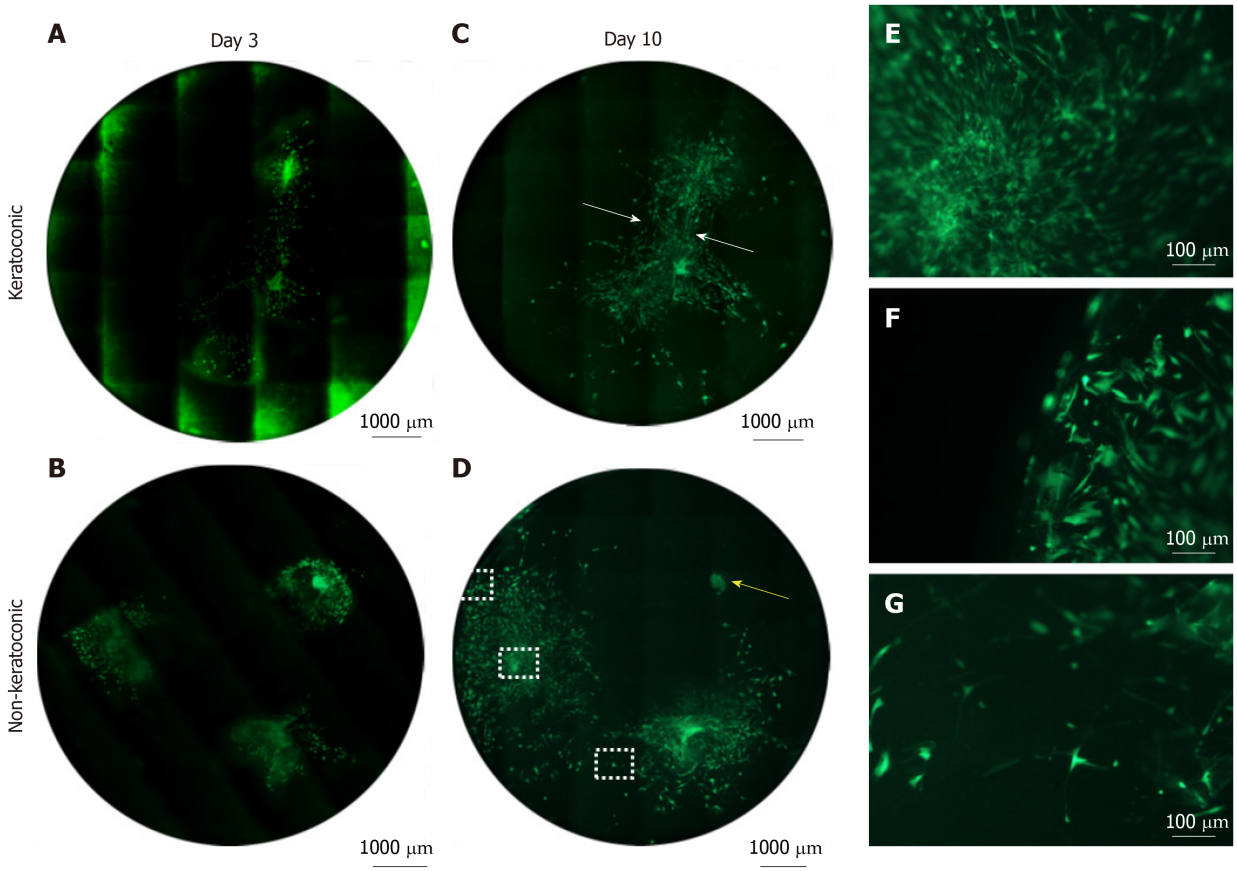

Figure 5 Cell viability of spheres and sphere-derived cells within implanted full-thickness corneal tissue. A-D: Decellularised full-thickness central corneal stromal tissues (corneal buttons) implanted with three spheres each and assessed for cell viability with Calcein-AM (green) were imaged at 50 × magnification with a fluorescence microscope and montaged to maintain detail of individual cells throughout the entire corneal button. Each circle represents the corneal button edge. Three days after implantation (day 3), spheres in keratoconic (A) and non-keratoconic (decompensated: normal anterior cornea with failed endothelium) (B) matrices are viable and have viable cells radiating from the sphere. At day 10, spheres in keratoconic (C) and non-keratoconic (D) matrices remain viable, and the viable cells have migrated further outward from the centre of the sphere. An exception to this was one sphere within non-keratoconic tissue, which showed reduced cell migration at day 10 compared with day 3 (yellow arrow, D); E-G: Panels E-G are magnified areas from D indicated by dotted squares (E = central square, F = top square, G = lower square). When spheres are implanted close to each other, cells align between them as if forming "cellular bridges" (white arrows, C). Cells near the centre of the sphere orientate radially from the centre of the sphere (E) while cells near the tissue edge are aligned parallel with the edge (F). Cells distant from both the nearest sphere and the tissue edge appear to lose their alignment (G). Scale bar = 1000 μm for A-D and 100 μm for E-G. Bright green fluorescence at left edge of tiles in montage (A) is artefactual.

From as early as the time of adherence (day 0), some cells in the sphere labelled positively for the myofibroblast marker, αSMA. The majority of migrated cells were negative for this marker over the course of four days in immunocytochemistry sections. This coincides with ddPCR data, which showed decreased expression of αSMA below the level at day 0 in keratoconic sections over 14 d in culture. There was increased expression of αSMA in samples from one sphere donor seeded onto normal tissue relative to day 0 that resulted in a high level of donor-donor variation on normal tissue for αSMA expression. Perhaps the spheres from this donor on day 0 had an unusually low expression of αSMA. Therefore, even small increases in αSMA expression in other samples appeared magnified relative to day 0, or possibly these spheres mounted a more aggressive wound healing response. Sphere-derived cell migration may represent an early phase of wound healing or may be a response similar to the migration of neural crest cells seen embryologically, which are also vimentin-positive from studies of mammalian and avian embryogenesis[39].

Expression of epithelial cell marker, keratin 3, was detected at very low levels in the majority of samples, and its expression significantly decreased over time in both tissue types. There was also significantly decreased temporal expression of laminin α1, which is associated with epithelial cells. Taken together, these findings suggest that the migrated cells were eliciting a stromal cell response on what was largely a stromal matrix.

Cells of varying morphology were occasionally seen in long-term tissue-seeded or implanted cultures, including what appeared to be cells with keratocyte-like morphology. However, detection of the keratocyte marker keratocan by ddPCR was

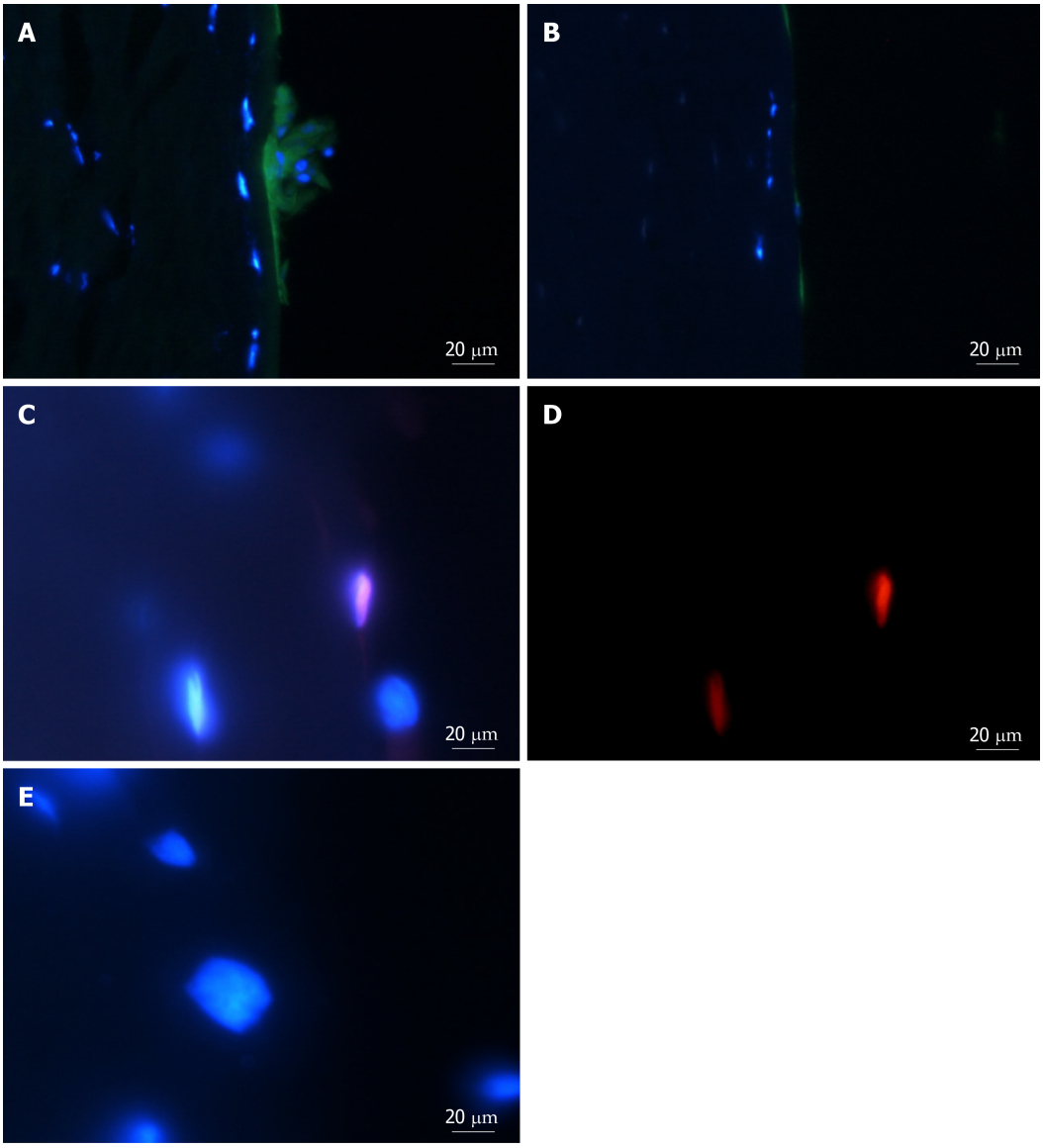

Figure 6 Putative stem-cell marker tumour protein p63, transcript variant 1, N-terminal isoform and cell-proliferation marker 5-ethynyl-2'-deoxyuridine in cells within sphere-implanted-full-thickness tissue at day 10. A: Representative images of cross sections with spheres and cells derived from spheres implanted into full-thickness keratoconic and non-keratoconic central corneal buttons at day 10 show positive staining within the sphere for the putative stem cell marker tumour protein p63, transcript variant 1, N-terminal isoform (ΔNp63α) (green); B: Cells stained without primary antibody (secondary antibody only control) show low green fluorescence. Cell nuclei are stained with DAPI (blue); C, D: Some, but not all cells show evidence of cell division (detected with ClickiT 5-ethynyl-2'-deoxyuridine (EdU) (red), a cell proliferation marker), as shown by pink cell nuclei in superimposed images of DAPI and EdU staining (C) and its equivalent image with red signal only (D); E: A negative control (EdU incubation without processing with its reaction solution) imaged at the same signal intensity as D is shown superimposed on DAPI for comparison. Scale bar = 20 μm.

significantly reduced over time and did not appear to support the differentiation of sphere cells into functioning keratocytes. It is likely that the 14-d duration of our repopulation experiments was too short for true keratocyte differentiation to be initiated. Similarly, we did not observe any consistent increase in collagen I production (neither α1 nor α2 chains), although there was an observed nonsignificant increase in expression of the alpha chain variant in keratoconic tissue but again with high donor-donor variation. The fact that we observed similar levels of collagen expression in keratoconic and normal tissue may indicate the beginnings of these cells laying down new matrix. Whether this would result in repair of the abnormal collagen matrix in keratoconic stroma remains to be seen. Longer term experiments may help in elucidating this.

Taken together, these results suggest that when spheres are implanted into or onto corneal stromal matrix, sphere-derived cells migrate and differentiate down a lineage appropriate to the matrix they are exposed to. Although there is evidence they can maintain a level of stemness after implantation, this ability appears to be impaired on keratoconic tissue. It may be that we are below the stem cell threshold required within

keratoconic tissue to retain stemness to a similar level to that of normal tissue that may indicate the need for implantation of more spheres in keratoconic corneas. Culture conditions would also play a role, in particular culture medium components such as growth factors would dictate whether cells take a certain path towards differentiation or not. Cells could be directed as to which trajectory to take: adult wound healing or foetal wound healing (for example by addition of cytokines like transforming growth factor β1 or β2 for the former or transforming growth factor β3 for the latter)[40].

In this study, we have relied upon the inherent properties of the spheres to detect the matrix onto which they are placed and react accordingly by producing cells of the correct lineage for that particular surface. In our observations, spheres react to the matrix in which they are placed, and this appears to stimulate differentiation of sphere-derived cells. As the identification of signalling molecules that drive differentiation of sphere cells placed onto corneal matrices was beyond the scope of this study, we currently do not have data on the specific signalling molecules that drive this differentiation in a specific direction and thus are relying more on the environmental cues that sphere cells receive. Although the use of signalling molecules to direct sphere cell differentiation along a specific path may be beneficial, the molecular interactions are highly complex and unlikely to be completely reproduced by a single or even a mixture of signalling molecules.

A migratory, rather than differentiation, response of spheres is consistently observed when spheres are cultured with serum-containing medium despite different types of collagen substrates[16,30]. Our results show that when cell signals are controlled, and normal cells are exposed to keratoconic matrix, cells do not change their behavioural response to the diseased matrix. This suggests that diseased matrix in itself may not perpetuate the pathogenic process of keratoconus. The combination of scar-promoting cell signalling, inept wound healing capability of keratoconic stromal cells and abnormal matrix are likely to feed each other in the cycle of its pathogenesis. It is likely that a treatment that utilises both normal cells and normal cell signals may be able to alter the trajectory of the healing process towards normal. There are already some promising results of scarless regeneration of ablated stroma in corneal mouse wounds[41].

Spheres are a suitable delivery system of stem cells

Spheres have previously been shown as a delivery system for stem cells into normal tissue matrix but not in diseased tissue, which differs morphologically[30]. There are a number of advantages of using spheres as the mode of stem cell delivery. Firstly, spheres contain a heterogeneous population of cells of both epithelial and stromal origin in a 3D format, which better simulates the *in vivo* niche. This may be useful to treat keratoconus, which has features of both epithelial and stromal cell dysfunction. Secondly, sphere-forming assays are commonly used retrospectively to identify stem cells[42], so spheres can be confidently used knowing undifferentiated cells are present. Thirdly, spheres are dynamic entities shown to be capable of reacting to their environment whilst maintaining themselves for up to 4 mo[16]. Finally, spheres can be transplanted as defined entities and have shown capability to repopulate the normal stromal ocular surface[30].

Although we did not look at immune rejection markers in our study because our host tissues were decellularised, this is an important consideration for further research in this field. An alternative to sphere-based stem cell delivery is transplantation of stem cells in the form of corneal limbal explants. Limbal explants have been successful in treating patients with limbal stem cell deficiency; these have their own limitations however. Autografts are more successful than allografts owing to the lower likelihood of immune rejection, but keratoconus is a bilateral disease and even in patients who appear to have a non-affected eye, they are likely to develop bilateral disease long-term[43]. Also, the genotype of the autograft will still remain keratoconic. Allografts, on the other hand, have a high risk of rejection. This has been shown in mice[44] and even in human leukocyte-antigen matched grafts. One study found that one-third of matched limbal grafts had failed at 5 years[45].

Sphere-based stem cell delivery also has some limitations that need to be considered. Firstly, the neurosphere assay, or any technique utilising culture with high concentrations of mitogens to expand stem cells, is unlikely to detect quiescent stem cells[42]. While this means that the stem cells in spheres are possibly not representative of the entire *in vivo* stem cell populations, this does not necessarily limit therapeutic application in tissue repair. Also, the quiescent stem cells may not be able to be rapidly expanded *in vitro* with mitogens, which is not ideal for therapeutic use. Secondly, spheres are not clones, so intersphere variations are an inherent limitation and even without factoring patient response, therapeutic efficacy of each sphere will be different. However, given that stem cell enriched peripheral corneal

spheres formed by sphere forming assay represent a way to apply a well-defined, known cell population, they may provide an improved method for treating corneal dystrophies like keratoconus.

Integrating stem cell implantation with current treatments

For spheres to be used for tissue repair with good functional outcomes, several factors need to be considered and compared to keratoplasty, the current definitive treatment. Safety factors such as tumorigenic potential and immune compatibility, practicality factors such as method of delivery and tissue availability, and therapeutic factors such as efficacy and sustainability of treatment need to be considered.

We have demonstrated the ability of spheres to perceive the environment they are exposed to and respond to it accordingly. This has been evidenced by spheres respecting artefactual gaps in tissue sections, their alignment with tissue section edges as well as differentiation into cells appropriate to the matrix they are implanted on. Previous studies have also shown that spheres implanted into limbal matrix preferentially migrate onto cornea over sclera. Moreover, unlike oncogenic cells, spheres respond to signals given to them. Unrestricted cell growth from spheres therefore seems unlikely.

Owing to the relatively immunoprivileged status of the cornea and reduced rejection rates from avoiding breach of the corneal endothelium[1], introduction of spheres into the corneal stroma is likely to have a low risk of immune rejection. As with any allogenic transplant, human leukocyte antigen matching may help to further mitigate risk of immune rejection.

Spheres are transplantable; they can successfully be surgically implanted into full-thickness corneas and adhere relatively reliably within 30 min. While direct implantation could be one possible method of sphere delivery, alternative routes could be explored. Spheres and sphere-derived cells have demonstrated preference for collagen over plastic, so sphere-coated contact lenses may be an alternative. Amniotic membrane could also potentially be used, as it has been successfully used as a mode of delivery for limbal explants.

Compared to keratoplasty, spheres have the advantage of being able to utilise limited resource donor tissue to potentially treat more people as many spheres can be generated from a single donor corneo-scleral rim.

Cells can migrate up to 5 mm away from the central sphere in 14 d and contain actively dividing cells. These features mean that spheres can potentially be implanted at a single or a few points and not necessarily in most severely affected areas. Cells could migrate to the areas needed and multiple implants may not be needed as spheres possess the ability to divide and maintain themselves.

While spheres can repopulate a corneal tissue surface, studies into the potential interaction with native corneal cells and matrix production are necessary before their full therapeutic efficacy can be assessed. If decellularisation is necessary, spheres could potentially be introduced after corneal collagen cross-linking treatments.

We hypothesised that the improved outcome from keratoplasty compared to collagen cross-linking is likely due to the introduction of normal cells and matrix to the diseased cornea. We extrapolate this idea to propose that the introduction of normal cells alone would rehabilitate the keratoconic cornea, and the introduction of normal cells to a post collagen cross-linked cornea may also prove of benefit. We have shown that stem cell enriched spheres cultured in the laboratory from limbal cell extracts can be successfully seeded onto keratoconic *en face* tissue sections and implanted into full thickness central corneal tissue. We have confirmed the ability of these spheres to respond to diseased tissue in a similar way to their response to normal tissue and that the cells showed the correct markers and morphological tendencies for the tissue structures they were placed in. Spheres were able to repopulate the diseased tissue surface either partially or entirely with the number of spheres implanted appearing to be the only limitation to complete surface repopulation. Over 14 d, the cells remained in a largely migratory state but the cells showed the beginning of differentiation into the appropriate cell types. Longer term experiments coupled with the addition of appropriate cell signalling molecules may direct them towards a more regenerative state. Our findings indicate that the presence of diseased matrix does not appear to direct normal cells to behave abnormally and thus conversely normal cells implanted into diseased matrix may drive the repair of the matrix into a normal phenotype. These results are an important initial step towards the development of an enhanced treatment or perhaps even cure for keratoconus in the future.

ARTICLE HIGHLIGHTS

Research background
Keratoconus is a disease in which the front part of the eye, the cornea, becomes cone-shaped resulting in impaired vision. It is not clear why this disease occurs and why it progresses, although current treatments can help to improve vision. Reports in the literature of cross linking treatments that removed some of the native cells and strengthened the matrix, only halted or slowed the disease process for relatively short periods. On the contrary, transplanting healthy tissue containing healthy cells and matrix reduced recurrence rates. From this, we hypothesised that introducing healthy cells may be able to stop progression of the disease process. Stem cells possess many reparative and regenerative characteristics. Stem cell-enriched spheres cultured from healthy human corneal donors have been shown to be able to elicit healing responses and also can be implanted into normal corneal tissue to repopulate it. However, this regenerative ability of spheres has not previously been studied in diseased corneal tissue.

Research motivation
This study aimed to analyse how stem cell spheres behave in keratoconic tissue. It was not known whether stem cell spheres could survive or how they would behave when implanted into diseased corneal tissue. The eventual goal is to be able to use stem cell spheres for implantation and direct them to regenerate or repair diseased cornea with minimal invasiveness to donors and recipients.

Research objectives
Our research objectives were to implant stem cell spheres into keratoconic tissue and observe cell survival, proliferation, migration and differentiation. This data will inform the use of stem cell spheres for implantation into diseased tissue as a therapeutic tool.

Research methods
Spheres were implanted into full-thickness keratoconic tissues and also onto 10 μm thin slices of keratoconic stromal tissues. Similar implants were done in non-keratoconic tissues for comparison. Spheres were stained with the live cell stain Calcein-AM and imaged between days 0 and 14. Sphere implanted tissues were also analysed using indirect immunohistochemistry and droplet digital PCR.

Research results
Our results showed that spheres were able to survive to 14 d after being implanted into keratoconic and non-keratoconic tissues, both into full-thickness tissues as well as onto 10 μm tissue slices. There were no significant differences observed between how spheres migrated on keratoconic tissue compared to non-keratoconic tissue. Cells migrated from spheres radially and aligned with tissue edges. Cells were observed to increase in number with time by direct observation and by detection of cell proliferation markers. Putative stem cell markers were still detected 14 d post implantation but with lower levels of expression in the spheres implanted on keratoconic tissue compared to those implanted on normal tissue. Stromal cell markers increased while epithelial cell markers reduced indicating that spheres exhibit a response appropriate to the stimulus of stromal tissue. Future work will determine whether the cells will ultimately differentiate into keratocytes or how sphere-derived cells would progress *in vivo*.

Research conclusions
This study provided a novel insight into the implantation of healthy cells aimed at reducing disease progression in degenerative diseases like keratoconus. It has shown early insights into how spheres behave when implanted into diseased keratoconic corneal tissues. If healthy cells derived from implanted stem cell spheres can influence the diseased milieu into a healthier scenario, stem cell sphere implantation could be used to supplement corneal cross-linking procedures and delay the deterioration of vision for patients with keratoconus.

Research perspectives
This study informs the use of stem cell-enriched spheres as therapeutic agents in ocular tissue matrices. Future research would aim to study these interactions and how best to progress towards being able to use stem cells as a therapeutic adjunct to current treatments.

ACKNOWLEDGEMENTS
The authors want to thank both the people who donated their tissues and their families for their selfless contribution to this research. They would also like to acknowledge Judy Loh, Jeremy Mathan, Jacqui Ross, Wayne McCollough and Professor Charles McGhee from University of Auckland for advice and assistance with laboratory, technical, imaging, practical and translational aspects of this work, respectively.

REFERENCES
1 **Romero-Jiménez M**, Santodomingo-Rubido J, Wolffsohn JS. Keratoconus: a review. *Cont Lens Anterior*

Eye 2010; **33**: 157-66; quiz 205 [PMID: 20537579 DOI: 10.1016/j.clae.2010.04.006]
2 **Sherwin T**, Brookes NH. Morphological changes in keratoconus: pathology or pathogenesis. *Clin Exp Ophthalmol* 2004; **32**: 211-217 [PMID: 15068441 DOI: 10.1111/j.1442-9071.2004.00805.x]
3 **Somodi S**, Hahnel C, Slowik C, Richter A, Weiss DG, Guthoff R. Confocal in vivo microscopy and confocal laser-scanning fluorescence microscopy in keratoconus. *Ger J Ophthalmol* 1996; **5**: 518-525 [PMID: 9479549]
4 **Sherwin T**, Brookes NH, Loh IP, Poole CA, Clover GM. Cellular incursion into Bowman's membrane in the peripheral cone of the keratoconic cornea. *Exp Eye Res* 2002; **74**: 473-482 [PMID: 12076091 DOI: 10.1006/exer.2001.1157]
5 **Kenney MC**, Nesburn AB, Burgeson RE, Butkowski RJ, Ljubimov AV. Abnormalities of the extracellular matrix in keratoconus corneas. *Cornea* 1997; **16**: 345-351 [PMID: 9143810 DOI: 10.1097/00003226-199705000-00016]
6 **Erie JC**, Patel SV, McLaren JW, Nau CB, Hodge DO, Bourne WM. Keratocyte density in keratoconus. A confocal microscopy study(a). *Am J Ophthalmol* 2002; **134**: 689-695 [PMID: 12429244 DOI: 10.1016/s0002-9394(02)01698-7]
7 **Davidson AE**, Hayes S, Hardcastle AJ, Tuft SJ. The pathogenesis of keratoconus. *Eye (Lond)* 2014; **28**: 189-195 [PMID: 24357835 DOI: 10.1038/eye.2013.278]
8 **Wollensak G**. Crosslinking treatment of progressive keratoconus: new hope. *Curr Opin Ophthalmol* 2006; **17**: 356-360 [PMID: 16900027 DOI: 10.1097/01.icu.0000233954.86723.25]
9 **Raiskup-Wolf F**, Hoyer A, Spoerl E, Pillunat LE. Collagen crosslinking with riboflavin and ultraviolet-A light in keratoconus: long-term results. *J Cataract Refract Surg* 2008; **34**: 796-801 [PMID: 18471635 DOI: 10.1016/j.jcrs.2007.12.039]
10 **Kelly TL**, Williams KA, Coster DJ; Australian Corneal Graft Registry. Corneal transplantation for keratoconus: a registry study. *Arch Ophthalmol* 2011; **129**: 691-697 [PMID: 21320951 DOI: 10.1001/archophthalmol.2011.7]
11 **Bourges JL**, Savoldelli M, Dighiero P, Assouline M, Pouliquen Y, BenEzra D, Renard G, Behar-Cohen F. Recurrence of keratoconus characteristics: a clinical and histologic follow-up analysis of donor grafts. *Ophthalmology* 2003; **110**: 1920-1925 [PMID: 14522765 DOI: 10.1016/S0161-6420(03)00617-1]
12 **Chunyu T**, Xiujun P, Zhengjun F, Xia Z, Feihu Z. Corneal collagen cross-linking in keratoconus: a systematic review and meta-analysis. *Sci Rep* 2014; **4**: 5652 [DOI: 10.1038/srep05652]
13 **Mazzotta C**, Balestrazzi A, Traversi C, Baiocchi S, Caporossi T, Tommasi C, Caporossi A. Treatment of progressive keratoconus by riboflavin-UVA-induced cross-linking of corneal collagen: ultrastructural analysis by Heidelberg Retinal Tomograph II in vivo confocal microscopy in humans. *Cornea* 2007; **26**: 390-397 [PMID: 17457184 DOI: 10.1097/ICO.0b013e318030df5a]
14 **Garfias Y**, Nieves-Hernandez J, Garcia-Mejia M, Estrada-Reyes C, Jimenez-Martinez MC. Stem cells isolated from the human stromal limbus possess immunosuppressant properties. *Mol Vis* 2012; **18**: 2087-2095 [PMID: 22876135]
15 **Chen SY**, Hayashida Y, Chen MY, Xie HT, Tseng SC. A new isolation method of human limbal progenitor cells by maintaining close association with their niche cells. *Tissue Eng Part C Methods* 2011; **17**: 537-548 [PMID: 21175372 DOI: 10.1089/ten.TEC.2010.0609]
16 **Yoon JJ**, Wang EF, Ismail S, McGhee JJ, Sherwin T. Sphere-forming cells from peripheral cornea demonstrate polarity and directed cell migration. *Cell Biol Int* 2013; **37**: 949-960 [PMID: 23619932 DOI: 10.1002/cbin.10119]
17 **Joyce N**, Annett G, Wirthlin L, Olson S, Bauer G, Nolta JA. Mesenchymal stem cells for the treatment of neurodegenerative disease. *Regen Med* 2010; **5**: 933-946 [PMID: 21082892 DOI: 10.2217/rme.10.72]
18 **Phinney DG**, Prockop DJ. Concise review: mesenchymal stem/multipotent stromal cells: the state of transdifferentiation and modes of tissue repair--current views. *Stem Cells* 2007; **25**: 2896-2902 [PMID: 17901396 DOI: 10.1634/stemcells.2007-0637]
19 **Spees JL**, Olson SD, Whitney MJ, Prockop DJ. Mitochondrial transfer between cells can rescue aerobic respiration. *Proc Natl Acad Sci U S A* 2006; **103**: 1283-1288 [PMID: 16432190 DOI: 10.1073/pnas.0510511103]
20 **Wilson SE**, Liu JJ, Mohan RR. Stromal-epithelial interactions in the cornea. *Prog Retin Eye Res* 1999; **18**: 293-309 [DOI: 10.1016/S1350-9462(98)00017-2]
21 **Wilson SE**, He YG, Weng J, Li Q, McDowall AW, Vital M, Chwang EL. Epithelial injury induces keratocyte apoptosis: hypothesized role for the interleukin-1 system in the modulation of corneal tissue organization and wound healing. *Exp Eye Res* 1996; **62**: 325-327 [PMID: 8795451 DOI: 10.1006/exer.1996.0038]
22 **Arnal E**, Peris-Martínez C, Menezo JL, Johnsen-Soriano S, Romero FJ. Oxidative stress in keratoconus? *Invest Ophthalmol Vis Sci* 2011; **52**: 8592-8597 [PMID: 21969298 DOI: 10.1167/iovs.11-7732]
23 **Buddi R**, Lin B, Atilano SR, Zorapapel NC, Kenney MC, Brown DJ. Evidence of oxidative stress in human corneal diseases. *J Histochem Cytochem* 2002; **50**: 341-351 [PMID: 11850437 DOI: 10.1177/002215540205000306]
24 **Mackiewicz Z**, Määttä M, Stenman M, Konttinen L, Tervo T, Konttinen YT. Collagenolytic proteinases in keratoconus. *Cornea* 2006; **25**: 603-610 [PMID: 16783151 DOI: 10.1097/01.ico.0000208820.32614.00]
25 **Cheung IM**, McGhee CNJ, Sherwin T. Deficient repair regulatory response to injury in keratoconic stromal cells. *Clin Exp Optom* 2014; **97**: 234-239 [PMID: 24147544 DOI: 10.1111/cxo.12118]
26 **Ma Y**, Xu Y, Xiao Z, Yang W, Zhang C, Song E, Du Y, Li L. Reconstruction of chemically burned rat corneal surface by bone marrow-derived human mesenchymal stem cells. *Stem Cells* 2006; **24**: 315-321 [PMID: 16109757 DOI: 10.1634/stemcells.2005-0046]
27 **Bray LJ**, Heazlewood CF, Munster DJ, Hutmacher DW, Atkinson K, Harkin DG. Immunosuppressive properties of mesenchymal stromal cell cultures derived from the limbus of human and rabbit corneas. *Cytotherapy* 2014; **16**: 64-73 [PMID: 24094499 DOI: 10.1016/j.jcyt.2013.07.006]
28 **Zhu WZ**, Van Biber B, Laflamme MA. Methods for the derivation and use of cardiomyocytes from human pluripotent stem cells. *Methods Mol Biol* 2011; **767**: 419-431 [PMID: 21822893 DOI: 10.1007/978-1-61779-201-4_31]
29 **Huang SU**, Yoon JJ, Ismail S, McGhee JJ, Sherwin T. Sphere-forming cells from peripheral cornea demonstrate a wound-healing response to injury. *Cell Biol Int* 2015; **39**: 1274-1287 [PMID: 26094955 DOI: 10.1002/cbin.10501]
30 **Mathan JJ**, Ismail S, McGhee JJ, McGhee CN, Sherwin T. Sphere-forming cells from peripheral cornea demonstrate the ability to repopulate the ocular surface. *Stem Cell Res Ther* 2016; **7**: 81 [PMID: 27250558 DOI: 10.1186/s13287-016-0339-7]

31 **Mathan J**, Ismail S, McGhee J, Sherwin T. Implantation of Human Peripheral Corneal Spheres into Cadaveric Human Corneal Tissue. *Bio Protoc* 2017; **7**: e2412 [DOI: 10.21769/BioProtoc.2412]

32 **Nolan T**, Hands RE, Ogunkolade W, Bustin SA. SPUD: a quantitative PCR assay for the detection of inhibitors in nucleic acid preparations. *Anal Biochem* 2006; **351**: 308-310 [PMID: 16524557 DOI: 10.1016/j.ab.2006.01.051]

33 **Bates D**, Mächler M, Bolker B, Walker S. Fitting Linear Mixed-Effects Models Using lme4. *J Stat Softw* 2015; **67**: 1-48 [DOI: 10.18637/jss. v067. i01]

34 **The R Core Team**. R: A Language and Environment for Statistical Computing; Version 3.6.1, 2019. Available from: URL: https://www.R-project.org

35 **Cheng EL**, Maruyama I, SundarRaj N, Sugar J, Feder RS, Yue BY. Expression of type XII collagen and hemidesmosome-associated proteins in keratoconus corneas. *Curr Eye Res* 2001; **22**: 333-340 [PMID: 11600933 DOI: 10.1076/ceyr.22.5.333.5491]

36 **Tuori AJ**, Virtanen I, Aine E, Kalluri R, Miner JH, Uusitalo HM. The immunohistochemical composition of corneal basement membrane in keratoconus. *Curr Eye Res* 1997; **16**: 792-801 [PMID: 9255508 DOI: 10.1076/ceyr.16.8.792.8989]

37 **Meek KM**, Tuft SJ, Huang Y, Gill PS, Hayes S, Newton RH, Bron AJ. Changes in collagen orientation and distribution in keratoconus corneas. *Invest Ophthalmol Vis Sci* 2005; **46**: 1948-1956 [PMID: 15914608 DOI: 10.1167/iovs.04-1253]

38 **Naylor RW**, McGhee CN, Cowan CA, Davidson AJ, Holm TM, Sherwin T. Derivation of Corneal Keratocyte-Like Cells from Human Induced Pluripotent Stem Cells. *PLoS One* 2016; **11**: e0165464 [PMID: 27792791 DOI: 10.1371/journal.pone.0165464]

39 **Bronner-Fraser M**, Stern CD, Fraser S. Analysis of neural crest cell lineage and migration. *J Craniofac Genet Dev Biol* 1991; **11**: 214-222 [PMID: 1725870]

40 **Karamichos D**, Zareian R, Guo X, Hutcheon AE, Ruberti JW, Zieske JD. Novel in Vitro Model for Keratoconus Disease. *J Funct Biomater* 2012; **3**: 760-775 [PMID: 23888249 DOI: 10.3390/jfb3040760]

41 **Basu S**, Hertsenberg AJ, Funderburgh ML, Burrow MK, Mann MM, Du Y, Lathrop KL, Syed-Picard FN, Adams SM, Birk DE, Funderburgh JL. Human limbal biopsy-derived stromal stem cells prevent corneal scarring. *Sci Transl Med* 2014; **6**: 266ra172 [PMID: 25504883 DOI: 10.1126/scitranslmed.3009644]

42 **Pastrana E**, Silva-Vargas V, Doetsch F. Eyes wide open: a critical review of sphere-formation as an assay for stem cells. *Cell Stem Cell* 2011; **8**: 486-498 [PMID: 21549325 DOI: 10.1016/j.stem.2011.04.007]

43 **Rabinowitz YS**, Yang H, Rasheed K, Li X. Longitudinal Analysis of the Fellow Eyes in Unilateral Keratoconus. *Invest Ophthalmol Vis Sci* 2003; **44**: 1311-1315

44 **Mills RA**, Coster DJ, Williams KA. Effect of immunosuppression on outcome measures in a model of rat limbal transplantation. *Invest Ophthalmol Vis Sci* 2002; **43**: 647-655 [PMID: 11867579]

45 **Reinhard T**, Spelsberg H, Henke L, Kontopoulos T, Enczmann J, Wernet P, Berschick P, Sundmacher R, Böhringer D. Long-term results of allogeneic penetrating limbo-keratoplasty in total limbal stem cell deficiency. *Ophthalmology* 2004; **111**: 775-782 [PMID: 15051212 DOI: 10.1016/j.ophtha.2003.07.013]

Published By Baishideng Publishing Group Inc
7041 Koll Center Parkway, Suite 160, Pleasanton, CA 94566, USA
Telephone: +1-925-3991568
E-mail: bpgoffice@wjgnet.com
Help Desk: https://www.f6publishing.com/helpdesk
https://www.wjgnet.com